Stereoblock Polypropylene from a Metallocene Catalyst with a Hapto-Flexible Naphthyl−Indenyl Ligand

Claudio De Rosa,* Finizia Auriemma, and Teresa Circelli

Dipartimento di Chimica, Università di Napoli "Federico II" Complesso Monte S. Angelo, Via Cintia, 80126 Napoli, Italy

Pasquale Longo and Antonella Caterina Boccia

Dipartimento di Chimica, Università di Salerno, Via S. Allende, I-84081 Baronissi (SA), Italy

Received November 14, 2002; Revised Manuscript Received March 20, 2003

ABSTRACT: Stereoblock polypropylenes have been obtained performing the polymerization of propene at different temperatures in the presence of [1-methyl-1-naphthylethyl-2-inden-1-yl]zirconium(IV) trichloride and methylaluminoxane. The stereoblock microstructure probably arises from to fact that the zirconium complex exists in equilibrium among structures having the naphthyl group coordinated to the metal, corresponding to chiral and/or pseudo-achiral forms, and a structure having the naphthyl group not coordinated, corresponding to a semimetallocene form. The chiral form produces regular isotactic sequences, whereas the pseudo-achiral and the semimetallocene forms produce atactic sequences, giving rise to isotactic−atactic stereoblocks. The length of the isotactic block depends on the polymerization temperature. A structural characterization and an analysis of the thermal behavior of these stereoblock polypropylenes have been performed. The samples crystallize from the melt in mixtures of α and γ forms of isotactic polypropylene. In the samples polymerized at low temperatures (17 and 30 °C), the amount of γ form is lower than that observed in samples prepared at higher temperatures (50 °C). This indicates that the regular isotactic sequences are longer in samples prepared at low temperatures, according with the interconversion mechanism of the catalyst among isospecific and aspecific forms. In these samples the amount of γ form is, in any case, lower than that observed in the literature for samples having higher stereoregularity and a random distribution of stereodefects, confirming the stereoblock microstructure of the samples prepared with the flexible catalyst.

Introduction

Stereospecific polymerization of α-olefins, in the presence of homogeneous catalytic systems based on substituted stereorigid group 4 *ansa*-metallocenes (precatalyst) and methylaluminoxane (cocatalyst), is largely self-explanatory due to the clear-cut relationship between the symmetry properties of the precatalyst and stereospecificity. In fact, polymerizing propylene in the presence of metallocenes of symmetry groups C_2, C_s, or C_{2v}, is possible to obtain isotactic, syndiotactic, or atactic polypropylene, respectively.[1−5]

Thus, a metallocene catalyst, derived from nonrigid unbridged bis(2-aryl-indenyl)zirconocenes, produces a polypropylene having a stereoblock microstructure consisting of consecutive blocks of isotactic and atactic sequences and that presents elastomeric behavior.[6] The stereoblock microstructure derives from an interconversion of the catalyst between chiral (isospecific) and achiral (aspecific) rotameric forms, during the course of the polymerization.[6−8]

Isotactic polypropylene can be also produced at low temperature, e.g. −60 °C, by C_{2v} titanocenes in the presence of methylaluminoxane (MAO) and the stereoregularity is due to *chain-end* control,[1,9,10] while stereoregular polypropylene is never obtained by using half-sandwich group 4 metal compounds.

Recently we obtained, in the presence of titanium trichloro[(1,2,3,4,5-η)-1-(1-methyl-1-phenylethyl)-2,4-cyclopentadien-1-yl] and at low reaction temperature (−60 °C),[11] partially isotactic polypropylene with chain-end control. ^{13}C NMR analysis has indicated that the sequence of configurations along the polymer chains is described by a first-order Markovian statistical model (the distribution of stereochemical diads was of Bernoulli type) with probability of formation of *m* diads $p_m = [m] = 0.77$. At high reaction temperature, we obtained nearly atactic polypropylene, $p_m = 0.51$.[11] This result was justified considering that, as showed by Sassmannshausen et al., complexes of titanium and zirconium with cyclopentadienyl−benzyl substituted give, at low temperature, aryl π-coordination to the metal, producing *ansa*-arene complexes, and, at high temperature, *half-sandwich* metallocenes.[12] Accordingly, the catalyst would behave, at low temperature, as a metallocene (e.g., Cp_2TiCl_2, Cp = cyclopentadienyl) producing isotactic polypropylene, via chain-end control mechanism,[1] and at high temperature, as a half-metallocene (e.g., $CpTiCl_3$), producing atactic polypropylene. The same catalytic system instead produces, at high temperature, syndiotactic polystyrene, which clearly originates from the half-metallocene form.[11] Moreover, in the presence of [1-methyl-1-naphthylethyl-2-inden-1-yl]zirconium(IV) trichloride **(LZrCl$_3$)**, as well as with the corresponding titanium compounds, we obtained metal controlled partially isotactic polypropylene.[11]

In this paper we report some results of the polymerization of propene in the presence of **LZrCl$_3$/MAO**, and the investigation that provides evidence for the presence of atactic − isotactic stereoblocks in the obtained polymer chain. A structural characterization of the obtained polypropylene samples, which supports the presence of a stereoblock microstructure, is reported. A new strategy for synthesizing elastomeric polypropene by using a catalyst whose structure switches between isospecific and aspecific configurations is suggested.

10.1021/ma021684t CCC: $25.00
Published on Web 04/19/2003

Table 1. Polymerization of Propene in the Presence of $LZrCl_3$/MAO Catalyst

run[a]	t (h)[b]	T (°C)	yields (g)	activity[c]
1	17.5	50	3.95	2.9×10^3
2	21	30	5.17	1.9×10^3
3	21	17	2.20	7.0×10^2

[a] All the runs were performed utilizing 100 mL of toluene, 20.0 μmol of $LZrCl_3$, 10.0 mmol of MAO (based on Al), under constant pressure of 5 atm of propene. [b] The productivity of the catalytic system was checked to be constant during the polymerization runs. After the first 5 min of polymerization the volume of the reaction mixture does not change, although the equilibrium concentration of the monomer in the solution is reached after longer time. [c] Activity = g of polymer/(mol of catalyst)(h)(mol/L of monomer).

Experimental Part

Reagents. Toluene was dried by refluxing over Na-diphenyl ketyl and distilling under a nitrogen atmosphere before use. Propene was purchased from Società Ossigeno Napoli; methylaluminoxane (MAO) was purchased from Witco and used as a solid after distillation of the solvent. [1-methyl-1-naphthylethyl-2-inden-1-yl]zirconium(IV) trichloride (**$LZrCl_3$**) was prepared according to the literature,[11] purified by crystallization from CH_2Cl_2, and further characterized by ^{13}C NMR analysis. ^{13}C NMR ($CDCl_3$): 23.1_2 and 25.1_6 ($C(CH_3)_2$); 26.5_4 ($C(CH_3)_2$); aromatic carbons 121.2_0 (*C*H); 121.2_5 (*C*H); 123.7_1 (*C*H); 123.9_5 (*quaternary carbon*); 124.9_3 (*C*H); 126.2_4 (*C*H); 126.4_7 (*quaternary carbon*); 127.8_2 (*C*H); 128.5_9 (*C*H); 132.3_1 (*quaternary carbon*); 134.4_0 (*quaternary carbon*); 135.7_6 (*quaternary carbon*); 136.8_8 (*quaternary carbon*). Anal. Calcd for $C_{22}H_{19}Cl_3Zr$: C, 54.94; H, 3.98; Cl, 22.11; Zr, 18.96. Found: C, 54.76; H. 4.12; Cl, 22.01; Zr, 19.11.

Polymerizations. All the runs were carried out in a 250 mL glass autoclave, thermostated at the temperatures reported in Table 1, introducing MAO (10.0 mmol, 580 mg) and **$LZrCl_3$** (20.0 μmol, 10 mg) dissolved in 100 mL of toluene. The autoclave was fed with propene (5 atm) and kept under magnetic stirring over the runs, then it was vented and the polymerization mixture was poured into acidified ethanol; the polymers were recovered by filtration, washed with fresh ethanol and dried in a vacuum at 80 °C. The polymerization conditions are reported in Table 1.

Fractionation. All the samples were dissolved in boiling heptane in a 500 mL pear-shaped-bottom flask, obtaining traces of insoluble fraction and a soluble fraction that was cooled to room temperature. The fraction soluble in boiling heptane was crystallized at room temperature obtaining a heptane-insoluble fraction (HR) and a soluble fraction at room temperature. The latter was concentrated removing the solvent in a vacuum and precipitated in methanol and then was further fractionated by exhaustive extraction with boiling diethyl ether in a Kumagawa extractor. A diethyl ether insoluble fraction (EI) and a diethyl ether soluble fraction (ES) were separated.

Crystallization Procedure. The HR fractions of the samples were isothermally crystallized from the melt at different temperatures. Compression molded specimens were melted at 180 °C and kept for 5 min at this temperature in a N_2 atmosphere; they were then rapidly cooled to the crystallization temperature, T_c, and kept at this temperature, still in a N_2 atmosphere, for a time t_c long enough to allow complete crystallization at T_c. The samples were then rapidly cooled to room temperature and analyzed by wide-angle X-ray diffraction and DSC. In the various isothermal crystallizations, the crystallization time t_c is different depending on the crystallization temperature. The shortest time is 24 h for the lowest crystallization temperatures and increases with increasing the crystallization temperature, up to 2 weeks for the highest crystallization temperatures.

Analysis. ^{13}C NMR spectra were obtained on an AM 400 Bruker spectrometer operating at 100 MHz. The samples were prepared by dissolving 10 mg of polymer into 0.5 mL of 1,1,2,2-tetrachlorodideuterioethane. The spectra were recorded at 80 °C using hexamethyldisiloxane (HMDS) as an internal chemical shift reference.

The calorimetric measurements were performed with a differential scanning calorimeter (DSC) Perkin-Elmer DSC-7 with scans at different heating rates in a flowing N_2 atmosphere.

X-ray powder diffraction patterns were obtained at room temperature with an automatic Philips diffractometer using Ni-filtered Cu Kα radiation.

The relative amount of crystals in the γ form present in our samples was measured from the X-ray diffraction profiles, as suggested by Turner-Jones et al.,[13] by measuring the ratio between the intensities of the $(117)_\gamma$ reflection at $2\theta = 20.1°$, typical of the γ form, and the $(130)_\alpha$ reflection at $2\theta = 18.6°$, typical of the α form: $f_\gamma = I(117)_\gamma/[I(130)_\alpha + I(117)_\gamma]$. The intensities of $(117)_\gamma$ and $(130)_\alpha$ reflections were measured from the area of the corresponding diffraction peaks above the diffuse halo in the X-ray powder diffraction profiles. The amorphous halo has been obtained from the X-ray diffraction profile of an atactic polypropylene, and then it was scaled and subtracted to the X-ray diffraction profiles of the melt-crystallized samples.

Table 2. Fractionation of the Polypropylenes Obtained by $LZrCl_3$/MAO[a]

run	fractions[b]	% wt	[*m*]	[*mmmm*]	T_m (°C)
1	HR	12.0	0.85	0.72	141
	EI	7.3	0.83	0.54	135
	ES	80.7	0.51	0.13	
2	HR	12.4	0.87	0.76	143
	EI	11.4	0.84	0.63	137
	ES	76.2	0.49	0.10	
3	HR	14.5	0.88	0.72	145
	EI	52.5	0.50	0.16	
	ES	33.0	0.49	0.12	

[a] The experimental conditions are reported in Table 1. The concentrations of the isotactic *m* dyad and *mmmm* pentad and the melting temperature T_m of the various fractions are reported. [b] HR = fraction insoluble in heptane at room temperature; EI, ES = fractions insoluble and soluble in boiling diethyl ether, respectively.

Results and Discussion

Microstructural Characterization. The polypropylene samples investigated in this study were produced at different temperatures in the presence of **$LZrCl_3$** and MAO. The conditions of polymerizations, performed at different temperatures and monomer concentrations, are reported in Table 1.

The samples were fractionated in boiling heptane and diethyl ether, and by crystallization in heptane at room temperature, according to the procedure described in the Experimental Section. A fraction insoluble in heptane at room temperature (HR) and ether-soluble (ES) and ether-insoluble (EI) fractions were obtained. In Table 2, the results of the fractionation are reported.

GPC analyses of the fractions indicates a monomodal distribution of molecular weights, with rather large polydispersities (for instance, the molecular weights of the *EI* fractions of samples 2 and 3 are $M_w = 1.8 \times 10^5$, with $M_w/M_n = 4.2$, and $M_w = 7.6 \times 10^4$, with $M_w/M_n = 5.5$, respectively.

All the fractions were analyzed by ^{13}C NMR spectroscopy, showing a very different tacticity. In fact, isotactic pentad contents [*mmmm*] of the fractions span a considerable range and vary from 0.10 to 0.76 (see Table 2).

In Figure 1, the methyl regions of ^{13}C NMR spectra of the HR, EI, and ES fractions of sample 2 are reported. The ES fraction (Figure 1c) is substantially atactic, while the HR fraction (Figure 1a) presents a consider-

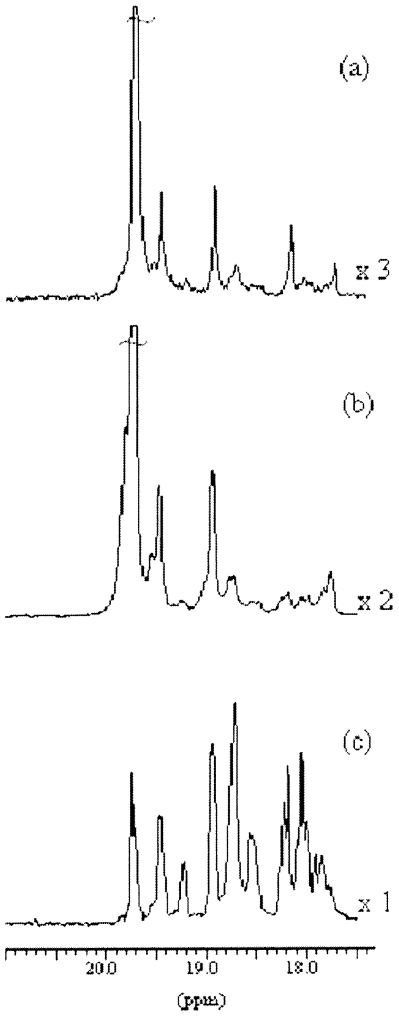

Figure 1. Methyl region of the ^{13}C NMR spectra of HR (a) (3-fold vertical expansion), EI (b) (2-fold vertical expansion), and ES (c) fractions of sample 2.

able amount in isotactic pentads. In the methyl region of the HR and EI fractions (Figure 1a,b) we were also able to detect the resonances of the *mmmrmr* and *mmrmrm* heptads that are diagnostic for chemical junctions between isotactic and stereoirregular blocks. These peaks become practically undetectable in the quasi-atactic fraction (Figure 1c). The experimental concentrations of these heptads (0.024, 0.010, respectively) are different from those calculated by utilizing an enanthiomorphic site (both 0.010), as well as a chain end type (both 0.025) statistical models.

In Table 3, are reported, as an example, the experimental stereosequence pentads concentrations of EI and HR fractions of sample 2. They are not in agreement with those calculated either by utilizing a statistical enantiomorphic site model or a Bernoullian model. Therefore, the stereoregularity of the polypropylene produced by the catalytic system **LZrCl$_3$** is not due to a stereospecific catalyst and is not produced by the steric control of the last inserted monomeric unit. The bad fitting could be justified considering a change in the structure of the catalytic site during the polymerization run.

These data suggest that the catalytic system [1-methyl-1-naphthylethyl-2-inden-1-yl]zirconium(IV) trichloride/MAO is able to produce isotactic−atactic stereoblocks polypropylene, probably because the zirconium

Table 3. Experimental and Calculated Concentrations of Pentad Stereorequences of EI and HR Fractions of Sample 2

			calcd	
fraction	stereosequence	exptl	enantiomorphic site model[a]	chain end control model[b]
EI	*mmmm*	0.631	0.634	0.666
	mmmr	0.110	0.121	0.142
	rmmr	0.008	0.006	0.008
	mmrr	0.114	0.121	0.015
	mmrm + *rrmr*	0.044	0.038	0.146
	mrmr	0.012	0.013	0.015
	rrrr	0.020	0.006	
	rrrm	0.020	0.013	0.002
	mrrm	0.041	0.060	0.008
HR	*mmmm*	0.758	0.774	0.801
	mmmr	0.044	0.081	0.091
	rmmr	0.017	0.002	0.003
	mmrr	0.062	0.081	0.005
	mmrm + *rrmr*	0.025	0.013	0.092
	mrmr	0.016	0.005	0.005
	rrrr	0.026	0.002	
	rrrm	0.023	0.005	
	mrrm	0.028	0.041	0.003

[a] Optimized values corresponding to σ (probability of insertion of the monomer with the right enantioface) equal to 0.913 (EI fraction) and 0.950 (HR fraction). [b] Optimized values corresponding to p_m (probability of formation of *m* diads) equal to 0.904 (EI fraction) and 0.946 (HR fraction).

complex is hapto-flexible and the catalytic system can be isospecific or aspecific depending on the naphthyl group, which may be coordinated or not to the metal. It is worth noting that the stereospecific structure of the catalytic complex depends on the oxidation state of the metal. If the oxidation state of zirconium was III, the complex could exist in equilibrium among three forms, shown in Scheme 1. In the two forms 1a and 1c, the naphthyl group is coordinated to the metal, whereas in form 1b the naphthyl group is not coordinated. Form 1a is chiral and produces isotactic sequences, whereas the form 1c is pseudo-achiral and produces atactic sequences. Atactic sequences can be derived also by the half-metallocene form 1b. The pseudo-achiral form 1c is probably not necessary to explain the formation of atactic sequences, but it is reasonable to assume that, as in the case of CH_2(1-indenyl)$_2ZrCl_2$, which exists in the *racemo*- and *meso*-forms,[5] the species of Scheme 1 may also exist in the pseudo-*racemic* form 1a and the pseudo-*meso* form 1c. Likewise, if the oxidation state of zirconium was IV, the metal would be pentacoordinate, when the naphthyl group is bound, or tetracoordinate when the naphthyl group is not bound to the metal. Pentacoordinate and tetracoordinate forms would produce isotactic and atactic polypropylene, respectively.

The results of the ^{13}C NMR analysis and the large distribution of the molecular weights indicate that the structure of the catalyst probably changes during polymerization;[8] the different catalytic species produce sequences of different tacticities, and polymer chains of different molecular weights. A fast interconversion of the catalyst between different forms would produce a narrow distribution of molecular weights. At variance, if different and noninterconverting catalytic species were present, a large, nonmonomodal distribution of molecular weights would be produced. The observed large monomodal distribution of molecular weights indicates that the catalytic species probably interconvert at intermediate rate, producing stereoblock polymer.

Structural Characterization. The polymorphic behavior of isotactic polypropylene (iPP) samples prepared

Scheme 1

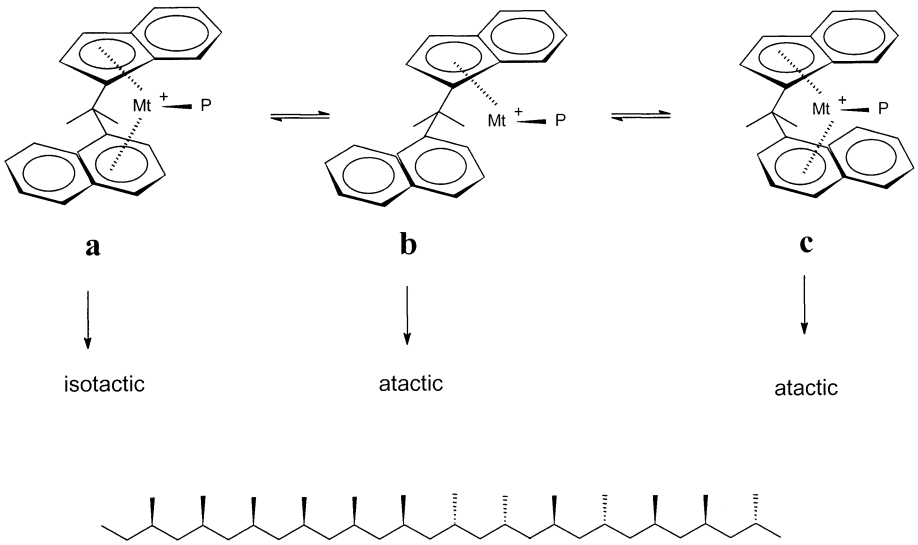

with single-center metallocene catalysts has been recently described.[14−21] In particular, it has been reported that in these samples the relative stability of the α and γ forms of iPP, under common conditions of crystallization, is completely different from that of iPP samples prepared with heterogeneous catalysts, and is closely related to their microstructure.[15,20,21]

Commercial iPP, prepared with the traditional heterogeneous Ziegler−Natta catalytic system, generally crystallizes in the stable α form.[22] The γ form may be obtained only under special conditions, i.e., by crystallization from the melt at elevated pressures (about 5000 atm)[22,23] or by crystallization at atmospheric pressure of low molecular weight samples[24] and of copolymers containing small amounts (in the range 5−20 mol %) of other olefins.[25]

iPP samples prepared with homogeneous metallocene catalysts crystallizes more easily in the γ form, even at atmospheric pressure and for high molecular weight samples.[14−20] The different polymorphic behavior of iPP samples prepared with heterogeneous and homogeneous catalysts is related to the different distribution along the chains of defects of stereo- and regioregularity, generated by the different kinds of catalytic systems. The distribution of defects, in turn, influences the average length of the crystallizable (fully isotactic) sequences.

The studies published so far[14−24] indicate that when the fully isotactic sequences are very short, iPP crystallizes in the γ form, whereas very long regular isotactic sequences generally crystallize only in the α form. In the chains of iPP samples prepared with homogeneous metallocene catalysts the distribution of defects is random and the length of fully isotactic sequences is roughly inversely related to the content of errors. As a consequence, even a small amount of defects reduces the length of the regular isotactic sequences and the γ form crystallizes.[14,15,18−21] In the case of iPP samples obtained with heterogeneous Ziegler−Natta catalytic systems, instead, a relatively large amount of defects may be segregated in a small fraction of poorly crystallizable molecules, so that longer fully isotactic sequences can be produced, leading to the crystallization of the α form even for a relatively high overall concentration of defects.[22]

It has been shown that for iPP samples prepared with metallocene catalysts, mixtures of the α and γ forms are generally obtained by isothermal crystallization from the melt,[14,15,18,20,21] and the content of γ form increases with increasing the content of defects.[15,18,20,21] The formation of the γ form seems to be favored by the presence of defects of stereoregularity (mainly *rr* isolated triads)[15,21] and/or regioregularity (mainly 2,1- and 3,1-insertions)[14,15] and also by the presence of constitutional defects, like comonomeric units.[17,18]

The kind of distribution of defects along the polymer chains also influences the crystallization of the γ form. It has been recently shown[20] that in the case of stereoblock polypropylene, prepared with oscillating unbridged metallocene catalysts,[6] the amount of γ form which develops in the melt-crystallization procedures, is much lower than that obtained for iPP samples having the same overall concentration of defects, but prepared with stereorigid metallocene catalysts, which produce a random distribution of defects.[20] This has been explained considering that in the stereoblock polypropylene most of the defects are segregated in stereoirregular (atactic), noncrystallizable blocks, which alternate to more regular isotactic sequences, long enough to crystallize in the α form.[20] This result has indicated that the maximum amount of γ form, which develops in iPP samples through melt-crystallization procedures, may provide indirect evidences of the presence of stereoblocks. An empirical method to establish the degree of segregation of defects along polypropylene chains has been, indeed, suggested.[20]

On the basis of these results, the polymorphic behavior of the iPP samples of Table 1, prepared with **LZrCl$_3$**, has been analyzed in order to evaluate the amount of γ form which crystallizes from the melt, and to give other evidences of the stereoblock nature of these polypropylenes.

The HR fractions of samples 1, 2, and 3 of Table 2 have been isothermally crystallized from the melt at different temperatures.

The X-ray powder diffraction profiles of the HR fractions of samples 1, 2, and 3 and of the samples isothermally crystallized from the melt at different temperatures are reported in the Figures 2−4, respectively. We recall that the α and the γ forms of iPP

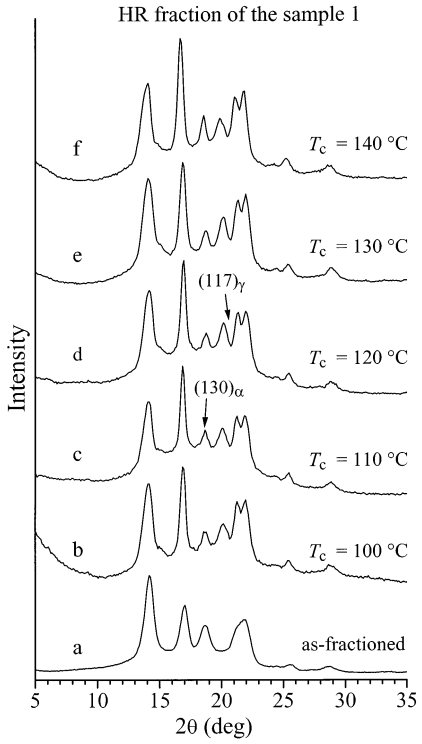

Figure 2. X-ray powder diffraction patterns of the fraction HR of the iPP sample 1 (curve a) and of specimens of the same fraction isothermally crystallized form the melt at the indicated temperatures. The $(130)_\alpha$ and $(117)_\gamma$ reflections at $2\theta = 18.6$ and 20.1°, respectively, typical of the α and γ forms of iPP, respectively, are also indicated.

present similar X-ray diffraction profiles, the main difference being the position of the third strong diffraction peak, which occurs at $2\theta = 18.6°$ ($(130)_\alpha$ reflection) in the α form[26] and at $2\theta = 20.1°$ ($(117)_\gamma$ reflection) in the γ form.[27,28] The presence of the diffraction peak at $2\theta = 18.6°$ and the absence of the reflection at $2\theta = 20.1°$ in the X-ray diffraction patterns of the fractions HR of the three samples (profiles a in Figures 2−4) indicate that these samples are basically in the α form.

It is apparent from Figures 2−4 that the diffraction patterns of the melt-crystallized samples of the HR fractions present both $(130)_\alpha$ and $(117)_\gamma$ reflections, indicating that a certain amount of γ form develops by crystallization from the melt. The relative intensity of the $(117)_\gamma$ reflection of the γ form at $2\theta = 20.1°$, with respect to that of the peak of the α form at $2\theta = 18.6°$ ($(130)_\alpha$ reflection), increases with increasing the crystallization temperature, reaches a maximum value, and then decreases for a further increase of the crystallization temperature. Moreover, it is apparent from Figures 2−4 that in the case of the HR fractions of samples 2 and 3, the amount of γ form, indicated by the intensity of the $(117)_\gamma$ reflection, is very low at any crystallization temperature, whereas sample 1 presents an amount of γ form significantly higher.

The relative amount of the γ form with respect to the α form, f_γ, for the various samples of the HR fractions is reported in Figure 5 as a function of the crystallization temperature. The content of the γ form increases with increasing the crystallization temperatures and a maximum amount of the γ form is obtained, for each sample, at temperatures in the range 120−130 °C.

These data are compared in the plot of Figure 5 with the amount of γ form obtained for iPP samples prepared with a single-center metallocene catalytic

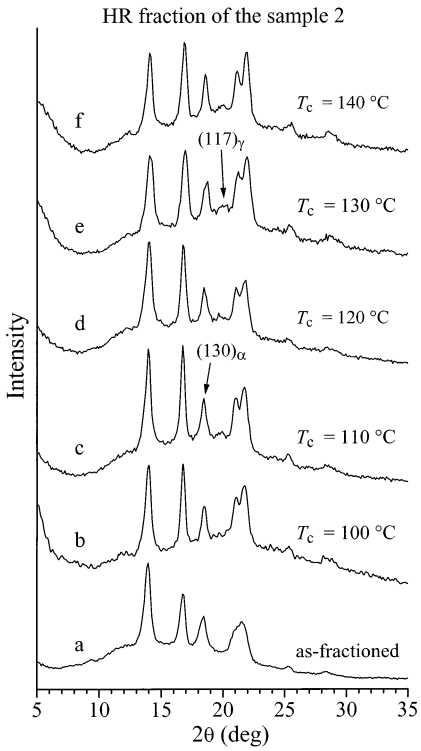

Figure 3. X-ray powder diffraction patterns of the fraction HR of the iPP sample 2 (curve a) and of specimens of the same fraction isothermally crystallized form the melt at the indicated temperatures. The $(130)_\alpha$ and $(117)_\gamma$ reflections at $2\theta = 18.6$ and 20.1°, respectively, typical of the α and γ forms of iPP, respectively, are also indicated.

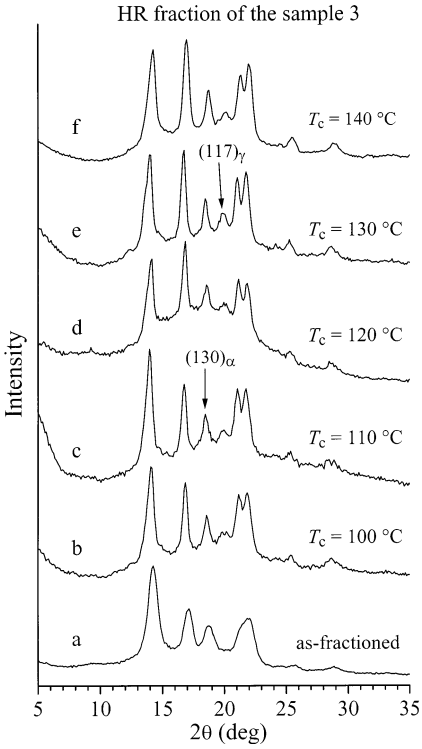

Figure 4. X-ray powder diffraction patterns of the fraction HR of the iPP sample 3 (curve a) and of specimens of the same fraction isothermally crystallized form the melt at the indicated temperatures. The $(130)_\alpha$ and $(117)_\gamma$ reflections at $2\theta = 18.6$ and 20.1°, respectively, typical of the α and γ forms of iPP, respectively, are also indicated.

system *rac*-isopropyliden[bis(3-trimethylsilyl)(indenyl)]-$ZrCl_2$/MAO (samples R1, R2 and R3 in Figure 5), taken

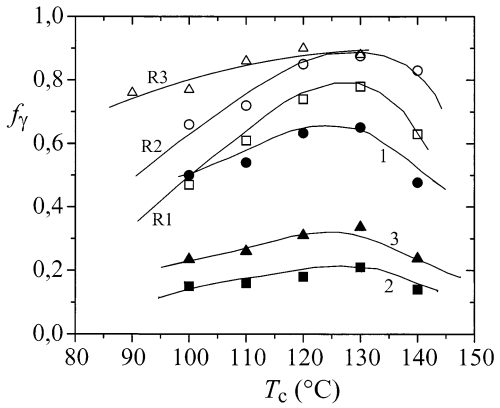

Figure 5. Content of the γ form, f_γ, evaluated from the X-ray diffraction profiles of the HR fraction of samples 1, 2, and 3 isothermally crystallized from the melt, as a function of the crystallization temperature, T_c. A comparison with the data reported in the literature,[21,22] relative to the content of γ form obtained for iPP samples prepared with *rac*-isopropyliden[bis-(3-trimethylsilyl)(indenyl)]$ZrCl_2$/MAO catalytic system (samples R1, R2, and R3), containing a random distribution of defects of stereorgularity, is shown. Key: (●) HR fraction of sample 1, [*mmmm*] = 72%; (■) HR fraction of sample 2, [*mmmm*] = 76%; (▲) HR fraction of sample 3, [*mmmm*] = 72%; (□) sample R1, [*mmmm*] = 89%; (○) sample R2, [*mmmm*] = 87.4%; (△) sample R3, [*mmmm*] = 83.4%.

from refs 20 and 21. As described by Resconi et al.,[29] this catalyst produces iPP samples characterized by chains containing only defects of stereoregularity (mainly isolated *rr* triads), whose amount depends on the polymerization temperature. The distribution of defects along the chains is random and no defects of regioregularity are present. This catalyst may be, therefore, taken as a reference catalyst for the single-center metallocene catalysts, because it produces very simple chain microstructure. As shown in refs 20 and 21, and in Figure 5, for these samples the content of γ form increases with increasing crystallization temperature and increases with increasing concentration of defects of stereoregularity. These data have indicated that the crystallization of the γ form is favored in iPP samples characterized by short regular isotactic sequences.[20,21] The lower the degree of isotacticity, the higher the maximum amount of the crystallized γ form (f_γ(max)), evaluated from the maxima of the curves of Figure 5. In particular, f_γ(max) ≈ 78% for sample R1 ([*mmmm*] = 89.0%) and 90% for the less stereoregular samples R2 and R3 ([*mmmm*] = 87.4 and 83.4%, respectively).[20,21]

Similar behavior is observed in Figure 5 for the HR fractions of samples 1, 2 and 3, with a notable difference in the maximum amount of the crystallized γ form. In fact, f_γ(max) ≈ 60% for the HR fraction of sample 1 ([*mmmm*] = 72.0%)], f_γ(max) ≈ 20% for the HR fraction of sample 2 ([*mmmm*] = 76.0%)] and f_γ(max) ≈ 30% for the HR fraction of sample 3 ([*mmmm*] = 72.0%)].

It is apparent from the comparison of Figure 5 that, the content of the γ form present in samples R1−R3 is always higher than that in samples 1−3, whatever the crystallization temperature, even though samples R1−R3 are more stereoregular than samples 1−3, and contain a lower concentration of defects.

As shown in refs 20 and 21, the relative stability of α and γ forms of iPP is related to the average length of the fully isotactic sequences in the chains comprised between two successive interruptions. The number of interruptions depends, in turn, on the content of defects and the degree of segregation of the defects along the polymer chain. Since samples R*i* have a random distribution of configurational errors (mainly isolated *rr* triads), the average length of the fully isotactic sequences,$\langle L_{iso}\rangle$, is inversely proportional to the content of errors ($\langle L_{iso}\rangle = 1/[rr]$). As a consequence, the amount of the γ form at a given crystallization temperature turns out to be higher for the less stereoregular sample R3 (with $\langle L_{iso}\rangle$ = 29 monomeric units) than for samples R2 ($\langle L_{iso}\rangle$ = 38 monomeric units) and R1 ($\langle L_{iso}\rangle$ = 43 monomeric units).[20,21] Samples 1, 2, and 3 have a higher concentration of defects than those of samples R*i* but a lower amount of the γ form; they, therefore, behave as if the average length of the fully isotactic sequences was longer than that in sample R*i*, even though their overall amounts of the fully isotactic pentads [*mmmm*] are lower than those of the samples R*i*. This indicates that in the HR fractions of samples 1, 2, and 3 the distribution of defects along the polymer chains is not random. The defects would be segregated in more stereoirregular or atactic sequences alternating to long isotactic or more stereoregular ones, giving rise to polymer chains with a stereoblock structure. The more isotactic sequences tend to crystallize in the α form and the amount of the γ form turns out to be low even though the overall degrees of stereoregularity, as evaluated by the ^{13}C NMR spectra, are apparently very low.

The three fractions HR of samples 1, 2, and 3 present a similar stereoregularity (Table 2) but the amount of the γ form crystallized for sample 1 (f_γ(max) ≈ 60%) is notably higher than those of the samples 2 and 3. This indicates that, even though sample 1 presents a strereoblock structure, the average length of the isotactic blocks is shorter than that in samples 2 and 3. This result seems in agreement with the mechanism of polymerization based on the equilibrium among the three forms of the catalytic complex, shown in the Scheme 1. The time that the catalyst spends in each of the three forms depends on the polymerization temperature. Sample 1 has been prepared at a higher polymerization temperature (50 °C); in this condition it is reasonable assuming that the catalyst spends less time in the isospecific chiral form with the naphthyl group coordinated to the metal. The average length of the isotactic sequences would be lower than in the case of the other two samples polymerized at lower temperature, in agreement with the higher amount of γ form developed in the melt-crystallizations. However, it is apparent from Figure 5 that the HR fraction of sample 3, prepared at the lowest temperature (17 °C), presents a slightly higher amount of γ form than that of sample 2, according to the lower stereoregularity (Table 2, [*mmmm*] = 76 and 72% for the HR fractions of samples 2 and 3, respectively). This behavior could be explained considering that at very low temperature the achiral mesolike form of the catalyst with the naphthyl group coordinated to the metal is probably slightly more stable than the isospecific racemolike form, or also, the insertion rate of the monomer is probably too slow with respect to the interconvertion rate of the catalyst between aspecific and isospecific forms.

A rough evaluation of the average length of the isotactic sequences in these stereoblock polypropylene may be obtained with the empirical method described in the ref 20, using the calibration plot of the maximum amount of the γ form, f_γ(max), as a function of the average length of the fully isotactic ...*mmmm*... se-

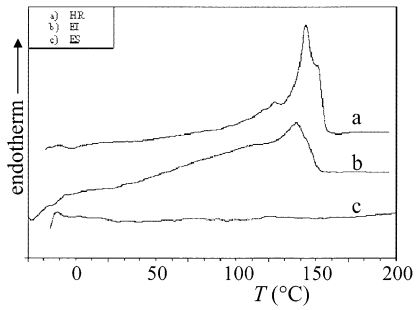

Figure 6. DSC curves of HR (a), EI (b), and ES (c) fractions of sample 2.

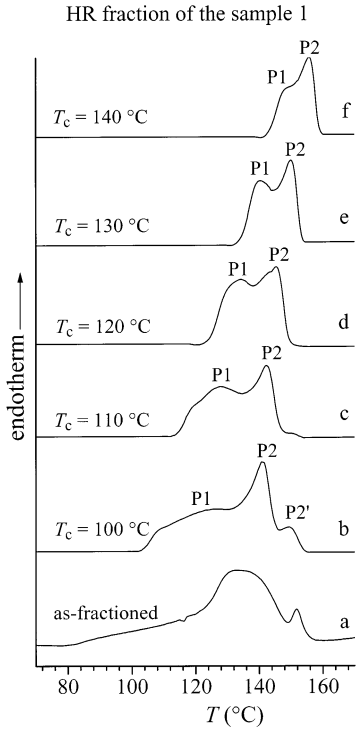

Figure 7. DSC curves at heating rate of 10 °C/min of the HR fraction of sample 1 and of specimens isothermally crystallized from the melt at the indicated temperatures.

quences $\langle L_{iso} \rangle$, obtained for iPP samples prepared with metallocene catalysts having a random distribution of defects. The average length of the fully isotactic sequences may be evaluated as $\langle L_{iso} \rangle = 1/\epsilon$, with ϵ the total concentration of errors determined by the ^{13}C NMR analysis. For these samples the maximum amount of γ form, which can be obtained for the various samples by the melt-crystallization procedures, is roughly linear with the logarithm of $\langle L_{iso} \rangle$ (see Figure 7 of ref 20). If this linear relationship is kept general whichever the distribution of defects, it is possible to find the length of the fully isotactic sequences also for stereoblock polypropylenes from the values of f_γ(max). The values of $\langle L_{iso} \rangle$ of 200, 150, and 50 monomeric units have been obtained for the HR fractions of samples 2, 3, and 1, respectively.

Thermal Analysis. Thermal analysis of the polypropylene samples and their fractions was carried out by differential scanning calorimeter. All the as-fractioned samples were heated to 250 °C, and after cooling to −50 °C at 10 °C/min, the samples were reheated to 250 °C at 10 °C/min. The melting temperatures of the fractions of the various polypropylene samples, measured from the last DSC run, are reported in Table 2. The DSC

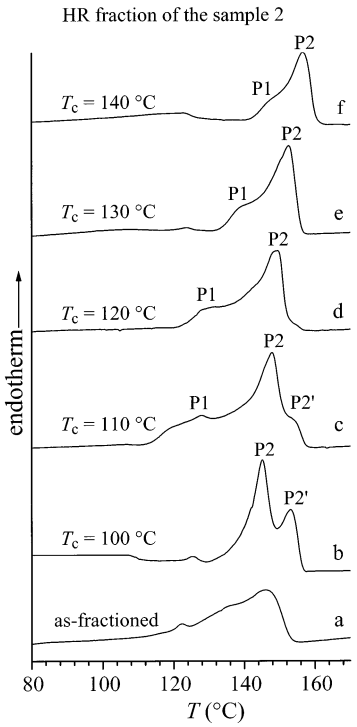

Figure 8. DSC curves at heating rate of 10 °C/min of the HR fraction of sample 2 and of specimens isothermally crystallized from the melt at the indicated temperatures.

heating curves of the fractions of sample 2 are reported in Figure 6 as an example. The fraction ES (Figure 6c) do not show any thermal transition under these experimental conditions, according with X-ray diffraction analysis, which indicates that the ES fractions of samples 1, 2, and 3 are basically amorphous. The DSC curves of EI (Figure 6b) and HR (Figure 6a) fractions display very broad endotherms with the onset of melting appearing below room temperature and continuing up to a peak ranging from 80 to 145 °C.

The DSC curves, recorded at 10 °C/min, of melt-crystallized samples of the HR fractions of samples 1, 2, and 3 are reported in Figures 7−9, respectively. A comparison with the DSC curves of the as-fractioned samples is also reported. It is apparent that all the as-fractioned samples present broad melting endotherms (curves a in Figures 7−9), corresponding to the melting of the α form, as indicated by the X-ray diffraction profiles of Figures 2−4 (curves a). In the case of sample 1 the melting endotherms shows multiple peaks, due, probably, to the occurrence of recrystallization of the α form crystals during the heating.

All the samples crystallized from the melt show melting endotherms characterized by double peaks, which have been indicated with P1 and P2 in Figures 7−9. The area of the peak at low temperature (P1) is low for samples 2 and 3, whereas it is relatively high for sample 1. Moreover, for the three samples it increases with increasing the crystallization temperature, up to T_c = 130 °C (curves e in Figures 7−9), then it decreases for a further increase of the crystallization temperature, as shown, for instance, for sample 1 in Figure 7 (curve f). The two peaks P1 and P2 are separated by nearly 30−40 °C in the DSC scans of the samples crystallized at low temperatures (for instance at T_c = 100 °C, curve b in Figure 9), but they approach each other at higher crystallization temperatures and are separated by less than 10 °C in the DSC scans of

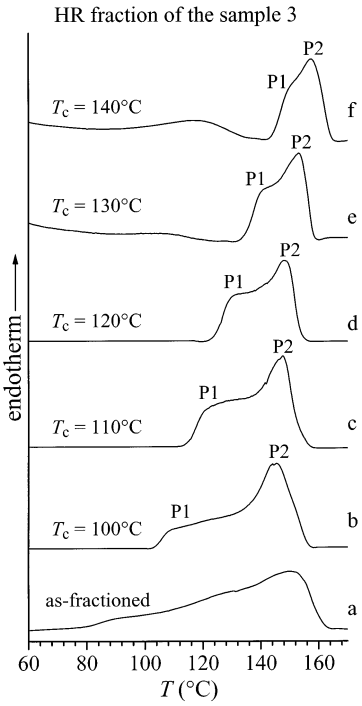

Figure 9. DSC curves at heating rate of 10 °C/min of the HR fraction of sample 3 and of specimens isothermally crystallized from the melt at the indicated temperatures.

the samples crystallized, for instance, at 140 °C (curves f in Figures 7 and 9). This indicates that the materials obtained at high crystallization temperatures melts in a more narrow range of temperature and that the crystals corresponding to the melting peak P1 are more improved than the crystals corresponding to the melting peak P2 with increasing crystallization temperature.

The melting behavior of these polypropylene samples is very similar to that described in the literature for other metallocene-made iPP samples crystallized from the melt.[15,20] In particular Alamo et al.[15] have shown that the multiple peaks present in the DSC scans are due to the melting of the α and γ forms of iPP, and that crystals of the γ form melt, generally, at lower temperatures. Recently, Auriemma and De Rosa[21] have shown that the lower melting temperature of the γ form is due to the presence in the γ form of structural disorder, and the large increase of the melting temperature of the γ form with increasing crystallization temperature, approaching the melting temperature of the α form crystals, is due to the decrease of the amount of structural disorder. These hypotheses could be valid also for our samples, which are characterized by mixtures of crystals of α and γ forms (Figures 3−5), even though the double peak shape of the endotherms in the DSC scans of Figures 7−9 could be also due, at least in part, to the occurrence of recrystallization phenomena during the heating. Therefore, in the DSC scans of Figures 7−9 the peak P1 could be due to the melting of the γ form, whereas the peak P2 is due to the melting of the α form.

To analyze the possibility of recrystallization, DSC scans were performed at different heating rates. DSC scans at different heating rates for some samples 1 and 2 are reported in Figures 10 as examples. It is apparent from Figure 10, parts A and C, that the relative area of the two melting peaks P1 and P2 do not change by changing the heating rate. This indicates that the two melting peaks P1 and P2 are not the result of the occurrence of recrystallization, but are mostly due to the melting of the crystals of two different polymorphic forms (γ and α forms, respectively), even though the occurrence of not relevant recrystallization phenomena cannot be excluded. It is apparent, however, that the DSC scans of Figures 7 (curve b), 8 (curves b and c), and 10B,C show that, in the samples crystallized at low temperatures the high-temperature peak P2 is split in two peaks, whose relative area change by changing the heating rate (Figure 10B,C). The area of the peak at higher temperature (P2′) decreases with increasing heating rate and almost disappears at 20 °C/min (Figure 10B,C). This indicates that the melting of the α form (peak P2) is generally associated with recrystallization phenomena. The DSC scans of Figures 7 and 8 clearly indicate that the amount of recrystallization decreases in samples crystallized at high temperatures. In these

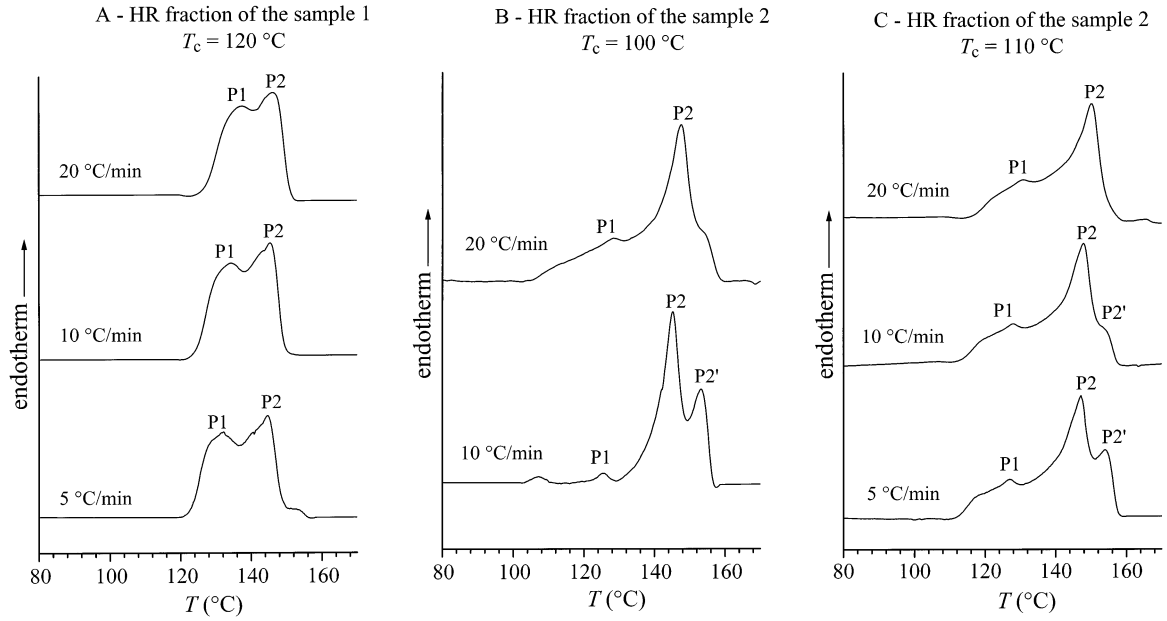

Figure 10. DSC curves recorded at different heating rates of the HR fraction of sample 1 crystallized from the melt at 120 °C (A) and of the HR fraction of sample 2 crystallized from the melt at 100 (B) and 110 °C (C).

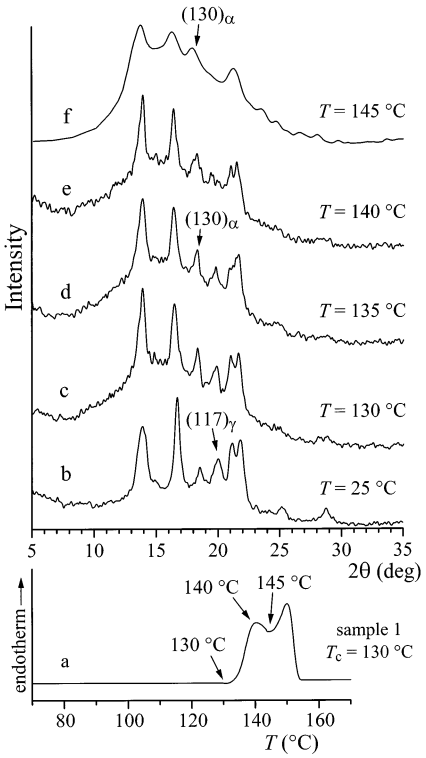

Figure 11. DSC scan, recorded at 10 °C/min, of the HR fraction of sample 1 isothermally crystallized form the melt at 130 °C (a) and X-ray powder diffraction profiles of the same sample recorded at the indicated temperatures (b−f). The $(130)_\alpha$ and $(117)_\gamma$ reflections at $2\theta = 18.6$ and 20.1°, respectively, typical of the α and γ forms of iPP, respectively, are also indicated.

samples, indeed, the peak P2 is no longer split and a melting endotherm of the α form with a single P2 peak is generally observed (curves c−f in Figure 7 and curves d−f in Figure 8).

The hypothesis that the peaks P1 and P2 are associated with the melting of γ and α forms, respectively, has been confirmed by the X-ray diffraction patterns of the melt-crystallized samples recorded at different temperatures. For instance, the diffraction profiles at different temperatures of sample 1 crystallized at 130 °C are reported in Figure 11. It is apparent that the intensities of the reflections of the γ form (mainly the $(117)_\gamma$ at $2\theta = 20.1°$) decrease progressively in the X-ray diffraction profiles recorded at high temperatures. At temperatures higher than the temperature corresponding to the melting peak P1 in the DSC scan (curve a in Figure 11), the $(117)_\gamma$ reflection disappears and only reflections of the α form are present (profile f in Figure 11). These data clearly indicate that the low-temperature peak P1 corresponds, basically, to the melting of the γ form, while the high-temperature peak P2 to the melting of crystals of the α form.

The results of the thermal analysis are in agreement with the structural analysis reported in the previous section. The suggested stereoblock microstructure of the HR fractions of the analyzed samples induces crystallization from the melt in mixtures of α and γ forms, the amount of the γ form being a function of the average length of the regular isotactic sequences. The γ form crystallizes in disordered modifications,[19−21] which always melt at temperatures lower than that of the α form. The amount of the γ form crystallized from the melt is higher for sample 1 synthesized at higher temperature (Figures 2 and 5), according to the short average length of the isotactic sequences and in agreement with the large area of the melting peak P1 in the DSC scans (Figure 7). The melting temperature of the crystals of the γ form strongly increases with increasing crystallization temperature, in agreement with the presence of disorder, whose amount decreases at high crystallization temperatures.

Conclusions

A catalytic system composed of [1-methyl-1-naphthylethyl-2-inden-1-yl]zirconium(IV) trichloride and methylaluminoxane has been utilized in the polymerization of propene at different temperatures. NMR analysis of the obtained samples has indicated that stereoblock polypropylene has been produced.

The stereoblock microstructure probably arises from the fact that the naphthyl group can be either coordinated or not coordinated to the metal, giving rise to complex species with different stereospecificities. If the oxidation state of zirconium was III, the complex would be in equilibrium among three forms. In two of the three structures the naphthyl group is coordinated to the metal, giving a chiral form and a pseudo-achiral form. In the third structure the naphthyl group is not coordinated, giving a semimetallocene form. The chiral form produces regular isotactic sequences, whereas the pseudo-achiral and the semimetallocene forms produce atactic sequences. The interconversion of the catalyst among the different species on a time scale comparable with the time required for monomer insertion, gives rise to isotactic−atactic stereoblocks. If the oxidation state of zirconium was IV, the catalytic species in equilibrium would be an isospecific *penta*coordinate complex (with the naphthyl group coordinated) and an aspecific *tetra*coordinated complex (with the naphthyl group not coordinated).

The structural characterization and the analysis of the thermal behavior of the polypropylene samples crystallized from the melt have confirmed the stereoblock microstructure. The samples crystallize from the melt in mixtures of α and γ forms of isotactic polypropylene. In the samples polymerized at low temperatures (17 and 30 °C), the amount of the γ form is lower than that observed in samples prepared at higher temperatures (50 °C). Since it has been reported that in metallocene-made isotactic polypropylene the γ form generally crystallizes when the regular isotactic sequences are short (for instance in samples containing an appreciable amount of defects of stereoregularity), the structural characterization indicates that in samples prepared at low temperatures the isotactic sequences are longer than those in the samples prepared at high temperatures. These data are in agreement with interconversion mechanism of the catalyst among isospecific and aspecific forms. At high temperatures the catalyst spends much time in the achiral semimetallocene form with the naphthyl group not coordinated to the metal, producing short regular isotactic sequences.

In these samples, the amount of γ form is, in any case, lower that that observed in the literature for iPP samples having higher stereoregularity and a random distribution of stereodefects, prepared with stereorigid isospecific C_2-symmetric metallocene catalyst.[20,21] This behavior confirms the stereoblock microstructure of the samples prepared with the flexible catalyst.

The analysis of the melting behavior of the stereoblock polypropylene samples is in agreement with the struc-

tural characterization. The DSC melting endotherms present multiple peaks corresponding to the melting of crystals of γ and α forms, at low and high temperatures, respectively. The lower melting temperature of the γ form is due to the presence of structural disorder in the γ form. However the melting temperature of the γ form strongly increases with the crystallization temperature, since the amount of disorder decreases with increasing crystallization temperature. The melting of the crystals of the α form is, generally, accompanied by recrystallization phenomena.

Acknowledgment. The authors wish to thank Dr. M. C. Costantino for the polymerization tests and Dr. P. Oliva for technical assistance. Financial support from the "Ministero dell'Università e della Ricerca Scientifica e Tecnologica" (PRIN 2002 and Cluster C26 projects) is gratefully acknowledged.

References and Notes

(1) Ewen, J. A. *J. Am. Chem. Soc.* **1984**, *106*, 6355.
(2) Kaminsky, W.; Kulper, K.; Brintzinger, H. H.; Wild, F. *Angew. Chem., Int. Ed. Engl.* **1985**, *24*, 507.
(3) Ewen, J. A.; Jones, R. L.; Razavi, A.; Ferrara, J. *J. Am. Chem. Soc.* **1988**, *110*, 6255.
(4) Brintzinger, H. H.; Fischer, D.; Mulhaupt, R.; Rieger, D.; Waymouth, R. M.*Angew. Chem., Int. Ed. Engl.* **1995**, *34*, 1143.
(5) Resconi, L.; Cavallo, L.; Fait, A.; Piemontesi, F. *Chem. Rev.* **2000**, *100*, 1253.
(6) Coates, G. W.; Waymouth, R. M. *Science* **1995**, *267*, 217.
(7) Petoff, J. L.; Agoston, T.; Lal, T. K.; Waymouth, R. M. *J. Am. Chem. Soc.* **1998**, *120*, 11316.
(8) Hauptman, E.; Waymouth, R. M.; Ziller, J. W. *J. Am. Chem. Soc.* **1995**, *117*, 11586.
(9) Zambelli, A.; Ammendola, P.; Grassi, A.; Longo, P.; Proto, A. *Macromolecules* **1986**, *19*, 2703.
(10) Zambelli, A.; Longo, P.; Ammendola, P.; Grassi, A. *Gazz. Chim. Ital.* **1986**, *116*, 731.
(11) Longo, P.; Amendola, A. G.; Fortunato, E.; Boccia, A. C.; Zambelli, A. *Macromol. Rapid Commun.* **2001**, *22*, 339.
(12) Sassmannshausen, J. *Organometallics* **2000**, *19*, 482.
(13) Turner-Jones, A.; Aizlewood, J. M.; Beckett, D. R. *Makromol. Chem.* **1964**, *75*, 134.
(14) Thomann, R.; Wang, C.; Kressler, J.; Mulhaupt, R. *Macromolecules* **1996**, *29*, 8425.
(15) Alamo, R. G.; Kim, M. H.; Galante, M. J.; Isasi, J. R.; Mandelkern, L. *Macromolecules* **1999**, *32*, 4050.
(16) VanderHart, D. L.; Alamo, R. G.; Nyden, M. R.; Kim, M. H.; Mandelkern, L. *Macromolecules* **2000**, *33*, 6078.
(17) Alamo, R. G.; VanderHart, D. L.; Nyden, M. R.; Mandelkern, L. *Macromolecules* **2000**, *33*, 6094.
(18) Thomann, R.; Semke, H.; Maier, R. D.; Thomann, Y.; Scherble, J.; Mulhaupt, R.; Kressler, J. *Polymer* **2001**, *42*, 4597.
(19) Auriemma, F.; De Rosa, C.; Boscato, T.; Corradini, P. *Macromolecules* **2001**, *34*, 4815.
(20) De Rosa, C.; Auriemma, F.; Circelli, T.; Waymouth, R. M. *Macromolecules* **2002**, *35*, 3622.
(21) Auriemma, F.; De Rosa, C. *Macromolecules* **2002**, *35*, 9057.
(22) Brückner, S. Meille, S. V.; Petraccone, V.; Pirozzi, B. *Prog. Polym. Sci.* **1991**, *16*, 361.
(23) Kardos, J. L.; Christiansen, W.; Baer, E. *J. Polym. Sci.* **1966**, *A-2* (*4*), 777. Pae, K. D.; Morrow, D. R.; Sauer, J. A. *Nature (London)* **1966**, *211*, 514. Pae, K. D. *J. Polym. Sci.* **1968**, *A-2* (*6*), 657. Sauer, J. A.; Pae, K. D. *J. Appl. Phys.* **1968**, *39*, 4959. Morrow, D. R. *J. Macromol. Sci., Phys. Ed.* **1969**, *B3*, 53.
(24) Lotz, B.; Graff, S.; Wittmann, J. C. *J. Polym. Sci., Polym. Phys.* **1986**, *24*, 2017. Kojima, M. *J. Polym. Sci.* **1967**, *5*, 245. Kojima, M. *J. Polym. Sci.* **1968**, *A-2* (*6*), 1255. Morrow, D. R.; Newman, B. A. *J. Appl. Phys.* **1968**, *39*, 4944.
(25) Turner-Jones, A. *Polymer* **1971**, *12*, 487.
(26) Natta, G.; Corradini, P. *Nuovo Cimento Suppl.* **1960**, *15*, 40.
(27) Brückner, S.; Meille, S. V. *Nature* **1989**, *340*, 455.
(28) Meille, S. V.; Brückner, S.; Porzio, W. *Macromolecules* **1990**, *23*, 4114.
(29) Resconi, L.; Piemontesi, F.; Camurati, I.; Sudmeijer, O.; Ninfant'ev, I. E.; Ivchenko, K. V.; Kuz'mina, L. *J. Am. Chem. Soc.* **1998**, *120*, 2308.

MA021684T